ELSEVIER

1 August 1996

Optics Communications 129 (1996) 62-68

OPTICS COMMUNICATIONS

Comparison of Tm-sensitized Ho:Yag and Ho:YLF crystals for a laser-pumped 2 μm CW oscillator

M. Tonelli [a], M. Falconieri [b], A. Lanzi [b], G. Salvetti [b,*], A. Toncelli [b,1]

[a] Dipartimento di Fisica, Università di Pisa, Piazza Torricelli 2, 50100 Pisa, Italy
[b] ENEA, CR Casaccia, Via Anguillarese 301, 00060 Rome, Italy

Received 24 November 1995; accepted 18 January 1996

Abstract

We report on a comparison of YAG and YLF crystals for Tm,Ho based CW laser systems operating at 2 μm. As pump source we have used both a Ti:Al_2O_3 laser and an array of diode lasers in order to quantitatively assess the relevance of the pump beam spatial features on the 2 μm laser performance. The results are compared with the predictions of a computer simulation using a rate equation model.

1. Introduction

The Ho emission near 2 μm has long been studied for the purpose of developing efficient devices for optical communications, coherent laser radar and detection of pollutants. This ion has been studied in different host crystals co-doped with Tm and operating either in CW or pulsed mode [1–10]. At present search is still actively being pursued for a host crystal that could optimize laser performance featuring reduced effects of the mechanisms that can limit the maximum achievable inversion ratio. In this experiment we compare the laser effect due to the Ho $^5I_7 \rightarrow {}^5I_8$ transition in YAG and YLF. These are two of the crystals which have been recognized among the most interesting ones, although none of them has yet emerged as the prime material.

In these co-doped systems the pump photons excite the $^3H_4$ multiplet of Tm. As a consequence of a cross-relaxation mechanism Tm ions are excited in the $^3F_4$ multiplet and, finally, an energy transfer process populates the $^5I_7$ Ho multiplet which is the upper laser level for the 2 μm emission. One of the primary attractive features of these systems resides in their suitability for diode laser pumping, offering the opportunity for the development of small compact laser systems. Nevertheless the spatial quality of the laser beam produced by diode laser, and in particular by diode laser arrays, is far from being ideally suitable for optimizing overlapping of the pump and laser mode volumes. Therefore a second aim of the work presented in this paper has been comparing the 2 μm laser behaviour under the conditions which characterize diode laser array pumping, with the behaviour corresponding to pumping by

* Corresponding author. Fax: +39-6-30484864; E-mail: salvetti@casaccia.enea.it.

[1] Present address: Dipartimento di Fisica, Università di Pisa, Piazza Torricelli 2, 50100 Pisa, Italy.

PII S0030-4018(96)00114-9

means of a $Ti:Al_2O_3$ laser capable of producing a high quality TEM_{00} beam.

We have also analyzed the 2 μm laser action in different operating conditions, by varying both the working temperature of the crystal near room temperature and the optical coupling geometry. Finally, we have compared some of the experimental results with the predictions of a macroscopic rate equation model. This work has been done in order to study the possibility of building a main oscillator for LIDAR applications.

2. Experimental apparatus

Two different crystals have been used as laser active media in this study. The concentrations of Tm and Ho ions in the crystals are 5.75% Tm, 0.3% Ho for the YAG crystal, and 5% Tm, 0.5% Ho for the YLF crystal. Both samples are cylindrical with a diameter of 5 mm and a length of 1.6 and 2.1 mm for the YAG and YLF crystal, respectively. The end-faces of the two crystals are polished flat and anti-reflection coated in order to have negligible losses both at 2 μm and at the pump laser wavelength. In particular, the reflectivity is < 0.2% at wavelengths between 2.05 and 2.1 μm, and < 2.0% at the 785–792 nm pump wavelengths.

The laser active media are placed in a nearly hemispherical optical cavity (Fig. 1). The flat resonator mirror transmits 95% of the laser pump radiation in the 790 nm wavelength region, and is a high reflector at 2 μm. The other mirror is curved and it serves as the output coupler transmitting ~ 0.5% of the laser radiation between 2.05 and 2.1 μm. The radius of curvature of this mirror is 10 cm and the two resonator mirrors are spaced by ~ 10 cm. The laser crystals sit in a copper mount on top of a thermoelectric cooler allowing their temperature to be varied from 0 to +40°C to test the laser performance under various working conditions. The mount and laser crystals are purged with dry nitrogen to minimize condensation, and one end of the crystal is ~ 1 mm from the flat mirror.

The 2 μm laser is longitudinally pumped with the output from either a $Ti:Al_2O_3$ laser or a diode laser array. In both cases the pump beam is focused by a lens which is placed in the proximity of the plane mirror. The $Ti:Al_2O_3$ laser is from Coherent (model 899-01) and it can deliver a power of up to 500 mW in the spectral region of interest, when pumped by a multiline Ar laser. The emission bandwidth of this laser is of about 0.1 nm. Its optical quality is quite good ($M^2 \sim 1.1$) with a nearly Gaussian output beam. Consequently the focused pump beam waist is nearly symmetrical.

The other pump laser is a Spectra Diode diode laser array (model SDL-2432-P1) which can deliver up to 1.2 W power with an emission bandwidth of approximately 2 nm. Some problems have been encountered for obtaining a proper profile of its beam in the interaction zone, because of the rectangular shape of the source. An aspheric lens (of 6 mm focal length) and two spherical mirrors (of 6 cm radius of

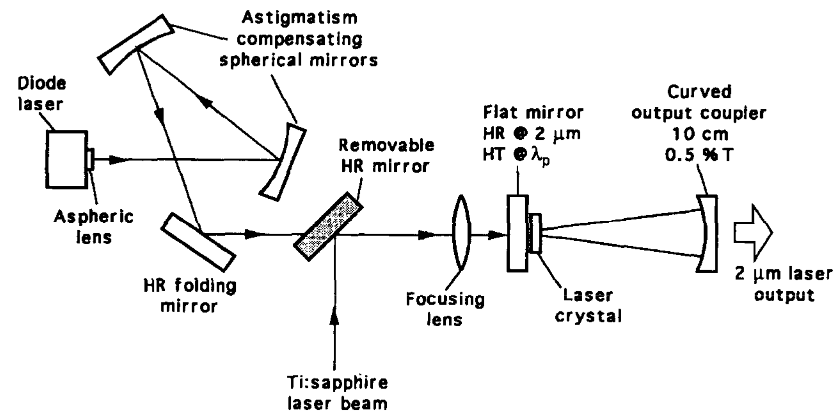

Fig. 1. Schematic of the resonator and pumping geometry used for the 2 μm laser characterization.

curvature) have been used to compensate for the astigmatism and the divergence of the output beam [11]. In this way the pump beam is finally focused to an elliptical spot of size approximately 100 × 25 μm in the laser crystal. The adopted optical geometry makes it feasible to pump the YLF crystal in the $\pi = (E \parallel c)$ configuration with both the pump lasers, while for the YAG crystal we have not selected any particular orientation since this crystal has a cubic symmetry.

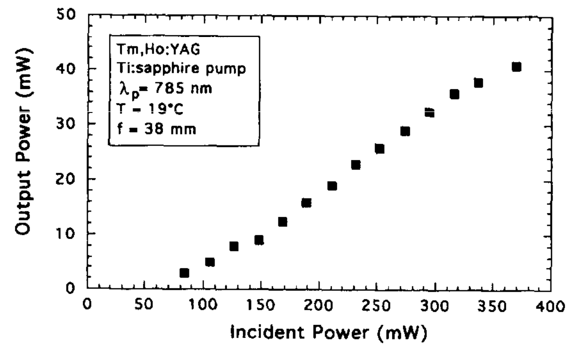

Fig. 3. Output power versus incident power for the Tm,Ho:YAG CW laser in the case of $Ti:Al_2O_3$ laser pumping.

3. Experimental results

Laser performance for the two different crystals can initially be compared in terms of the results obtained with the $Ti:Al_2O_3$ laser. The broad tunability range of this laser allows to use it for pumping at the wavelengths corresponding to the two highest absorption peaks of the Tm,Ho:YLF crystal, i.e. at 780 and 792 nm, and to the absorption peak of the Tm,Ho:YAG crystal at 785 nm. We have measured the 2 μm laser output at various temperatures between 0 and 20°C. In Fig. 2 we show typical curves of the output power versus power incident onto the YLF crystal at room temperature with a lens of focal length equal to 52 mm. The maximum output power was 70 mW with 370 mW incident power at 780 nm pump wavelength ($\alpha \sim 5$ cm^{-1}), with a corresponding slope efficiency of 21%. The corresponding threshold power was about 22 mW. By decreasing the crystal temperature down to 0°C, the slope efficiency did not appreciably change but the threshold power was reduced at 13 mW. By pumping on the weaker absorption peak at 792 nm ($\alpha \sim 4$ cm^{-1}) the slope efficiency decreased at 19% and 17%, with a threshold power of 16 and 26 mW, for operation at 0°C and room temperature, respectively. Laser performance has also been investigated as a function of the focal length of the focusing lens, i.e. as a function of the dimensions of the pump beam waist. The output power did not exhibit significant changes for focal lengths varying between 38 and 63 mm, while it decreased noticeably when the focal length exceeded 70 mm. As for the radius of the pump beam waist, it changes from about 23 μm with the shortest focal length to about 87 μm with the longest one. For this crystal the emission wavelength was 2.06 μm independently of the pump wavelength.

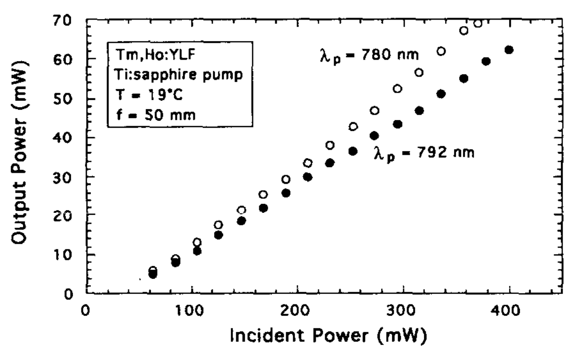

Fig. 2. Output power versus incident power for the Tm,Ho:YLF CW laser in the case of $Ti:Al_2O_3$ laser pumping at two different wavelengths.

As far as the YAG crystal is concerned, this crystal has been pumped at 785 nm, i.e. at the wavelength corresponding to the strongest absorption peak (with an absorption coefficient α equal to ~ 6 cm^{-1}) in the absorption band of interest. Radiation at this wavelength can easily be generated by both the pump lasers. In Fig. 3 we show the behaviour of the output power as a function of the incident power at room temperature in the case of $Ti:Al_2O_3$ laser pumping. The results reported here have been obtained with a focal length of the focusing lens equal to 38 mm for which the 2 μm power extraction was optimized. The highest measured output power is 40 mW for a 350 mW incident power, with a 14% slope efficiency and a threshold power of approximately 50 mW. Although the slope efficiency does not seem to vary by operating the crystal at 0°C, the threshold power decreases down to 26 mW at that temperature. The measured emission wavelength with the YAG crystal is 2.09 μm, which corresponds to the laser transition characterized by the highest net gain for this crystal.

From these results, it is evident that, under the operating conditions of our experiment, substantially better laser performance has been obtained with the YLF rather than with the YAG crystal. On the other hand it has to be noted that the Ho concentration in the YLF sample is significantly higher than that in the YAG sample and, moreover, it is well established that the emission cross-section of the laser transition is smaller in YAG than in YLF [12]. It has to be noted that the laser performance obtained in our experiment does not compare favourably with the best values reported so far. However some of the parameters which critically concur for maximizing the power extraction have not been optimized in our configuration. For example the laser is clearly under-coupled, but this solution has been adopted on purpose since it allows to investigate the laser behaviour under a quite large range of operating conditions.

Having characterized the laser performance under nearly ideal pumping beam conditions, we have investigated the effect of pumping with a diode laser array, quite attractive if one wishes to build very compact laser sources at 2 μm. The pumping geometry is like the one schematically shown in Fig. 1. For both the crystals we have used a 52 mm focal length lens, having verified the negligible effect on laser performance of the characteristics of this lens for focal lengths shorter than 70 mm. The diode laser array utilized in our experiment cannot operate at the 780 nm absorption peak of the Tm:YLF crystal. Consequently, the YLF and YAG samples have been pumped at 792 nm in the π configuration and at 785 nm, respectively.

Fig. 4 shows the results obtained at room temperature. The 2 μm laser with the YLF crystal exhibits a 14.4% slope efficiency, namely ~ 17% lower than the one obtained with the $Ti:Al_2O_3$ laser at the same pump wavelength. The maximum output power is 120 mW for an incident power of 950 mW with a threshold power of about 100 mW, significantly higher than that with the $Ti:Al_2O_3$ laser. We have also tested the laser at higher operating temperatures:

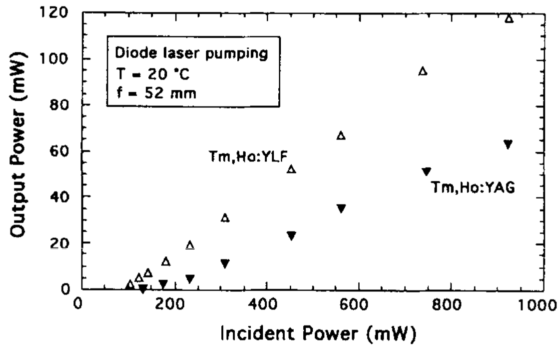

Fig. 4. Output power versus incident power for the Tm,Ho:YLF and the Tm,Ho:YAG CW lasers in the case of diode laser pumping. Pumping wavelengths are 792 and 785 nm for the YLF and YAG crystals, respectively.

laser action was still observed at 40°C, with a slope efficiency of 12% and a threshold power of about 150 mW. Even in the case of diode laser pumping, the use of the YAG crystal does not result in better laser performance: in fact, with this crystal operating at room temperature the system slope efficiency is 8.4%, with a maximum output power of 65 mW for a 950 mW incident power and a threshold power of about 130 mW. At 40°C the slope efficiency decreases down to 3.6% with a threshold power of about 280 mW.

As one can see, the results obtained with the diode laser are worse than those with the $Ti:Al_2O_3$ pump laser, at least as far as the slope efficiency and the threshold power are concerned. This result gives a clear quantitative indication of the importance of a good pump and laser mode volume overlapping for laser performance optimization, and it is not unexpected in our case. In fact, although we have made an attempt to improve the optical quality of the pump beam generated by the diode laser array, its waist is still highly asymmetrical with an ellipticity high enough to make practically impossible obtaining an optimized mode matching with the theoretical TEM_{00} Gaussian mode of the solid state laser. It is obvious that this affects unfavourably the efficiency of our 2 μm laser.

4. Performance simulation and discussion

The experimental results relative to the $Ti:Al_2O_3$-pumped Tm,Ho:YAG crystal have been compared with the predictions of a computer simulation of the laser characteristics based on a macroscopic rate equation model. This has been done having in mind a twofold aim: to get a deeper understanding of the mechanisms governing the laser oscillator behaviour, and to test and verify the accuracy of the model in order to use it as an aid for the design of optimized laser oscillators. Simulation of the laser performance for the YLF crystal has not been attempted, since it would require the use of rate parameters which are currently either unknown or ambiguously known. This is the case for most of the parameters which describe the energy transfer processes taking place among the Tm and Ho energy levels lying above the Tm $^3F_4$ and Ho $^5I_7$ multiplets. Nevertheless, direct or indirect determination of these parameters from experimental data is presently underway. As far as diode laser pumping is concerned, modelling of the laser behaviour under these conditions has not been considered since both the pump and laser transverse spatial profiles clearly showed a multitransverse mode nature that could not be accounted for in the model.

The rate equation model is based on the general framework of the quasi-three-level laser model proposed in Ref. [13]. In particular it assumes a Gaussian pump beam and single mode, lowest order (TEM_{00}), laser operation on a single transition, as it is reasonable for low-power oscillators. The model includes several types of radiative and nonradiative transitions among the various energy levels of the two trivalent rare earth ions. In particular, the model accounts for six fundamental processes, i.e. (i) cross-relaxation between Tm ions to populate the Tm $^3F_4$ manifold; (ii) energy transfer from and to the Tm $^3H_4$ and the Ho $^5I_5$ manifolds; (iii) energy transfer from and to the Tm $^3F_4$ and the Ho $^5I_7$ manifolds: (iv) Ho and Tm intra-centre de-excitation to the $^5I_8$ and $^3H_6$ ground manifolds, respectively; (v) upconversion to Ho $^5I_5$ involving the Tm $^3F_4$ and Ho $^5I_7$ states; and (vi) downward relaxation from high Ho^{3+} manifolds, i.e. the Ho $^5I_5$–$^5I_7$ manifolds, populated via energy transfer directly from the Tm $^3H_4$ manifold, or via upconversion. The model does not treat energy transfer between Tm^{3+} and Ho^{3+} ions as given by a Boltzmann distribution, since one of its aims is to account for the effects associated with depletion of the ground state manifolds. Thermal equilibrium analysis has just been used to derive the ratio of the Tm-to-Ho rate constants to that of Ho-to-Tm back transfer. Manifolds lying above the Tm $^3H_4$ and Ho $^5I_5$ have not been considered in the model since, as shown in the literature [14], the upconversion processes that excite the Tm^{3+} and Ho^{3+} ions to these states are relatively unimportant compared to the upconversion process (v) mentioned before. Regarding the input parameters for these processes, most of them were provided by the results of previous spectroscopic investigations carried out on the same crystal utilized as laser medium [15]. Geometrical parameters such as the pump and laser beam waists were determined by the experimental measurements performed on the laser. Finally the emission cross-section for the laser transition, the associated energy levels which enter the rate equations through their Boltzmann fractional populations, and

Table 1
Experimental and calculated values for relevant laser performance parameters, in the case of $Ti:Al_2O_3$ laser pumping of Tm,Ho:YAG laser. F is the focal length of the focusing lens, W_p and W_l are the radii of the pump and 2 μm laser beam waists, respectively; P_{th} is the threshold power

Experimental parameters					Model parameters				
					Input			Output	
F [mm]	W_p [μm]	W_l [μm]	P_{th} [mW]	Slope efficiency [%]	W_p [μm]	W_l [μm]	Losses [%]	P_{th} [mW]	Slope efficiency [%]
25	23 ± 1	39 ± 6	45 ± 2	12.3 ± 8	24	35	0.75	43	11.5
38	34 ± 1	33 ± 4	50 ± 2	14 ± 1	33	39	0.75	48	12.6
50	46 ± 2	45 ± 3	59 ± 2	12 ± 1	48	42	0.73	60	12.0
77	74 ± 3	43 ± 1	54 ± 2	12 ± 1	76	42	0.42	62	11.3

the cavity losses were used as free fitting parameters to be determined by a global comparison of the model predictions with experimental results on the laser oscillator. The set of experimental data used to set up and test the model consisted of all the threshold powers and slope efficiencies obtained at room temperature using different pump focusing lenses.

The obtained results are shown in Table 1. As can be seen, the model can reproduce rather well all the experimental data, although it tends to slightly underestimate the value of the slope efficiency for short focal lengths of the focusing lens. A possible cause for this may be that we have assumed the laser to oscillate on the same transition (and henceforth with the same emission cross-section) for each of the different pump beam waists. In particular the transition used in the model is the one occurring from the first level of the upper manifold to the twelfth level of the lower manifold, corresponding to a wavelength of 2.098 μm, with an associated stimulated emission cross-section of 8.5×10^{-20} cm^2. This value compares well with those reported in Refs. [2,12]. Nevertheless, the experimentally measured wavelength is compatible with a number of different transitions, the use of some of which (as for example the one occurring from the first level of the upper manifold to the twelfth level of the lower manifold) yields comparable results, even though for different values of the associated cross-section.

In any case the model seems to be capable of successfully simulating the relevant features of the experimental findings. Perhaps the major of these features is that optimized performance (at least in terms of threshold power) is achieved under conditions of relatively tight focused pumping beams, even though when the pump beam spot size dimensions become too small the laser slope efficiency is seen to decrease. By using the predictions of the computer simulation model, we have made clear that this behaviour might be attributed to the concomitant action of two different factors. The first consists in the mismatched dimensions of the pumping and laser mode volumes, and this has been experimentally observed. The second factor concerns the fact that the intracavity losses increase as the pumping volume dimensions decrease and this observation steps out only as a result of the computer simulation. This finding could be related to the higher criticalness in the optimization of the alignment of the optical components needed to reach a good overlapping between the pump and the laser beam.

5. Conclusions

We have reported some results of a comparative investigation of the performance of a 2 μm laser employing Tm,Ho co-doped different active crystals, namely YAG and YLF, operated near room temperature and pumped with two different laser pump sources, a high beam quality Ti:Al_2O_3 laser and a diode laser array. From this investigation emerges the relevance of a good overlapping of pumping and laser resonator volumes in order to optimize the laser performance. Quantitative comparison of the results obtained for both crystals under the two different pumping conditions may help for an assessment of the importance of this aspect.

Acknowledgements

One of the authors (AT) was supported by a grant from ENEA during this work.

References

[1] G. Huber, E.W. Duczynski and K. Petermann, IEEE J. Quantum Electron. 24 (1988) 920.
[2] T.Y. Fan, G. Huber, R.L. Byer and P. Mitzscherlich, IEEE J. Quantum Electron. 24 (1988) 924.
[3] A. Brenier, J. Rubin, R. Moncorge and C. Pedrini, J. Phys. (Paris) 50 (1989) 1463.
[4] H. Hemmati, Optics Lett. 14 (1989) 435.
[5] N.P. Bames and D.J. Gettemy, Appl. Optics 29 (1990) 404.
[6] A. Di Lieto, A. Neri, P. Minguzzi, F. Pozzi, M. Tonelli and H.P. Jenssen, in: Proc. Adv. Solid State Lasers, Eds. G. Dubè and L.L. Chase, Vol. 10 (Opt. Soc. Am., Washington DC, 1991) p. 213.
[7] G. Armagan, A.M. Buoncristiani, A.T. Inge and B. Di Bartolo, in: Proc. Adv. Solid State Lasers, Eds. G. Dubè and L.L. Chase, Vol. 10 (Opt. Soc. Am., Washington DC, 1991) p. 222.
[8] B.T. McGuckin and R.T. Menzies, IEEE J. Quantum Electron. 28 (1992) 1025.
[9] P.A. Budni, M.G. Knights, E.P. Chicklis and H.P. Jenssen, IEEE J. Quantum Electron. 28 (1992) 1029.
[10] R.R. Petrin, M.G. Jani, R.C. Powell and M. Kokta, Opt. Mater. 1 (1992) 111.

[11] A. Di Lieto, P. Minguzzi, A. Toncelli, M. Tonelli and H.P. Jenssen, Appl. Phys. B 58 (1994) 69.
[12] S.A. Payne, L.L. Chase, L.K. Smith, W.L. Kway and W.F. Krupke, IEEE J. Quantum Electron. 28 (1992) 2619.
[13] T.Y. Fan and R.L. Byer, IEEE J. Quantum Electron. 23 (1987) 605.
[14] M. Falconieri, A. Lanzi and G. Salvetti, Spectroscopic investigation of the visible and mid-infrared emission in Tm- and Ho-doped YAG and YLF crystals, Appl. Phys. B 62, accepted for publication.
[15] M. Falconieri and G. Salvetti, Optics Mater. 3 (1994) 157.